

Long-term fire effects on soil and vegetation nitrogen cycling: potential links to persistent stream nitrate export

 Allison E. Rhea^{A,*} , Timothy P. Covino^B and Charles C. Rhoades^C 

For full list of author affiliations and declarations see end of paper

***Correspondence to:**

Allison E. Rhea
 Colorado Forest Restoration Institute,
 Colorado State University, Fort Collins,
 CO, USA
 Email: Allison.Rhea@colostate.edu

Received: 5 June 2025
Accepted: 11 December 2025
Published: 6 February 2026

Cite this: Rhea AE *et al.* (2026) Long-term fire effects on soil and vegetation nitrogen cycling: potential links to persistent stream nitrate export. *International Journal of Wildland Fire* **35**, WF25145. doi:10.1071/WF25145

© 2026 The Author(s) (or their employer(s)). Published by CSIRO Publishing on behalf of IAWF.

This is an open access article distributed under the Creative Commons Attribution-NonCommercial 4.0 International License (CC BY-NC)

OPEN ACCESS

ABSTRACT

Background. Soil and stream nitrate (NO_3^-) concentrations often increase after severe fire from elevated nitrogen (N) mineralization and reduced plant uptake. However, it is unclear how long these effects persist and contribute to stream N export. **Aims.** We examined the contribution of soil N supply and vegetation N demand to 19-fold higher stream NO_3^- export that has persisted since the 2002 Hayman Fire in Colorado, USA. **Methods.** We compared soil N pools, inorganic N production, subsurface (0–100 cm) NO_3^- concentrations, vegetation cover, productivity and N demand 17 years post-fire. We sampled along burned and unburned hillslopes to evaluate whether near-stream vegetation and soils attenuated N loss during downslope transport. **Key results.** Mineral soil, leachate and groundwater NO_3^- concentrations were higher in burned than unburned hillslopes, despite similar mineralization rates. Burned uplands showed 62% lower productivity and 28% lower N demand relative to unburned forests. Riparian recovery exceeded uplands but remained incomplete relative to unburned conditions. Burned uplands acted as N sources, with slight reductions in soil NO_3^- in downslope riparian soils. **Conclusions.** Sustained NO_3^- export was driven by reduced vegetation N demand and subsurface transport, not increased mineralization. **Implications.** Revegetation of severely burned uplands and riparian zones may enhance long-term N retention.

Keywords: hillslope, hydrologic connectivity, nitrogen cycling, revegetation, riparian, topography, upland, wildfire.

Introduction

Terrestrial ecosystems are often limited by nitrogen (N), which is retained within undisturbed vegetation and soils (Chapin *et al.* 2011). Wildfires combust vegetation and surface organic matter, reduce biotic demand and can stimulate soil N mineralization and N-fixation (Hart *et al.* 2005; Johnson *et al.* 2005; Hanan *et al.* 2016b). Following severe wildfires, N-rich particulate materials such as ash, organic matter and mineral soil are mobilized by surface runoff (Lane *et al.* 2008; Pierson *et al.* 2019) and soluble nitrate (NO_3^-) may be transported along subsurface flowpaths (Murphy *et al.* 2006; Bladon *et al.* 2008). Elevated post-fire stream N can last years to decades and has been documented across western North America (Smith *et al.* 2011; Rust *et al.* 2018). Yet, most studies focus on short-term post-fire responses, creating uncertainty about which mechanisms maintain elevated watershed N export over longer time scales (e.g. > 10 years).

Wildfires commonly stimulate mineralization of organic soil N, though the duration of this response is uncertain. Organic matter pyrolysis can result in accumulation of ammonium (NH_4^+) in mineral soils (Covington and Sackett 1992; Wan *et al.* 2001). This, coupled with favorable soil temperature, moisture and pH promote the production of NO_3^- (e.g. nitrification), a mobile form of inorganic N susceptible to leaching (Bauhus *et al.* 1993; Hanan *et al.* 2016b). Short-term (< 5 years) post-fire increases in soil N mineralization and inorganic N are well documented (Wan *et al.* 2001; Dove *et al.* 2020), though nitrification can remain elevated for decades in some systems, such as the Arizona ponderosa pine forests in the USA (Kurth *et al.* 2014).

Rapid post-fire vegetation regrowth and nutrient uptake are known to mitigate N losses to streams (Turner *et al.* 2009; Dunnette *et al.* 2014). However, high severity wild-fire, combined with increasingly hot and dry post-fire conditions, has contributed to widespread declines in tree regeneration across western North America (Stevens-Rumann *et al.* 2018; Davis *et al.* 2019). This sparse regeneration suggests that recovery to pre-fire forest structure may take centuries (Chambers *et al.* 2016; Rother and Veblen 2016; Rhoades *et al.* 2025b), potentially prolonging suppressed vegetation N demand.

N cycling varies along topographic gradients due to interacting effects of soil, hydrology and vegetation. Following forest disturbance, upland soils often become sources of NO₃⁻, which leaches downslope to lower landscape positions and streams (Vitousek and Melillo 1979). In the Hayman fire scar, stream NO₃⁻ concentrations were highest below severely burned, convergent hillslopes (Rhea *et al.* 2022). This pattern is consistent with the role of topographic convergence in concentrating runoff and nutrients (McClain *et al.* 2003). In contrast, riparian zones often function as nutrient sinks that retain and transform upslope N inputs before they reach streams. Fine-textured soils, high moisture and abundant organic matter in these zones support vegetation uptake and promote microbial processes like denitrification, especially under saturated conditions (Lowrance *et al.* 1995; Dosskey *et al.* 2010). Similar to well-studied agroecosystems (Vidon and Hill 2004), riparian vegetation and soil microbes have been shown to retain over half of upland N losses following severe beetle outbreaks and salvage logging (Biederman *et al.* 2016; Rhoades 2018). Although wildfires often extend into riparian areas, sprouting shrubs and fire-resilient tree species often enable relatively rapid post-fire recovery (Dwire and Kauffman 2003). Understanding how riparian zones contribute to N retention is essential for predicting long-term nutrient transport in post-fire landscapes.

The 2002 Hayman Fire (Colorado, USA), offers a unique opportunity to investigate long-term N dynamics in watersheds where nearly two decades of water chemistry monitoring has shown persistent elevated stream N (Rhoades *et al.* 2011, 2019) and scarce post-fire tree regeneration (Chambers *et al.* 2016). More than a decade after the fire, NO₃⁻ export was 19-times higher in burned catchments, indicating substantially reduced watershed N retention (Rhoades *et al.* 2019). Based on these patterns, we hypothesized that elevated soil N mineralization and/or reduced vegetation N uptake drive the sustained post-fire N export. To test this, we sampled along burned and unburned hillslopes, extending from uplands to near-stream riparian zones, to assess how N availability changes with proximity to streams and whether near-stream soils and vegetation retain excess post-fire N. These findings advance understanding of long-term biogeochemical responses in severely burned watersheds and may inform post-fire revegetation strategies aimed at improving watershed health and surface water quality.

Methods

Site description

The 2002 Hayman Fire burned 550 km² of the Upper South Platte watershed, the primary drinking water supply to the nearby Denver metropolitan area. The study area fell within the lower montane zone of Pike National Forest which is dominated by ponderosa pine (*Pinus ponderosa*) and Douglas-fir (*Pseudotsuga menziesii*) (Kaufmann *et al.* 2000). About 65% of the fire burned at moderate to high severity and post-fire conifer regeneration density has been low in areas >50 m from live forest edges (Chambers *et al.* 2016). The fire increased understory plant richness and cover in uplands, driven by an increase in short-lived forbs (Fornwalt and Kaufmann 2014). *Bromus* spp., *Poa* spp., *Rosa woodsii*, *Rubus idaeus*, *Geranium* spp. and *Verbascum thapsus* dominated the understory at the time of our study.

All our study watersheds have a granitic lithology, underlain by Pike's Peak batholith (Ruleman *et al.* 2011). The batholith consists of medium to coarse-grained biotite and hornblende-biotite granite that weathers into coarse, sandy loam soils (i.e. Ustorthents and Cryorthents) (Moore 1992). Coarse fragments comprise 30% of the soil volume. At the time of our study, average pH was 6.3 in burned and 6.0 in unburned mineral soils.

On average, these study sites receive 280 mm of precipitation from snow and summer monsoonal rain each year (WRCC 2021) (Cheesman RAWs station, site ID: 053102, 1987–2022). The 2019 water year, when our sampling was conducted, was 60% drier than the historical average, with only 167 mm of precipitation (WRCC 2021). Stream discharge peaked in May during snowmelt though there were smaller rainfall-driven peaks throughout the late summer season (Supplementary Fig. S1). Atmospheric N deposition at our study sites was assumed to be relatively low (2.5–2.8 kg N/ha.year) based on elevation zones defined by Heindel *et al.* (2022). Higher deposition rates (4.4–4.7 kg N/ha.year) can occur at lower elevations (<1800 m) associated with major urban and agricultural areas along the Front Range of Colorado, highlighting the potential for spatial variability across the region (Heindel *et al.* 2022).

We measured several ecosystem N pools and fluxes at burned and unburned sites throughout the Hayman Fire (Fig. 1a). We focused on watersheds with extensive high severity fire, including sites where Rhoades *et al.* (2019) reported 19-fold higher mean annual NO₃⁻ export compared to nearby unburned streams (0.56 vs 0.03 kg N/ha.year). Importantly, pre-fire NO₃⁻ concentrations were similar across burned and unburned watersheds and between granitic and mixed lithology basins (Rhoades *et al.* 2011), strengthening the attribution of post-fire differences to fire effects rather than background variability. Export estimates were based on systematic water chemistry sampling that does not capture individual storm events. While storm-driven

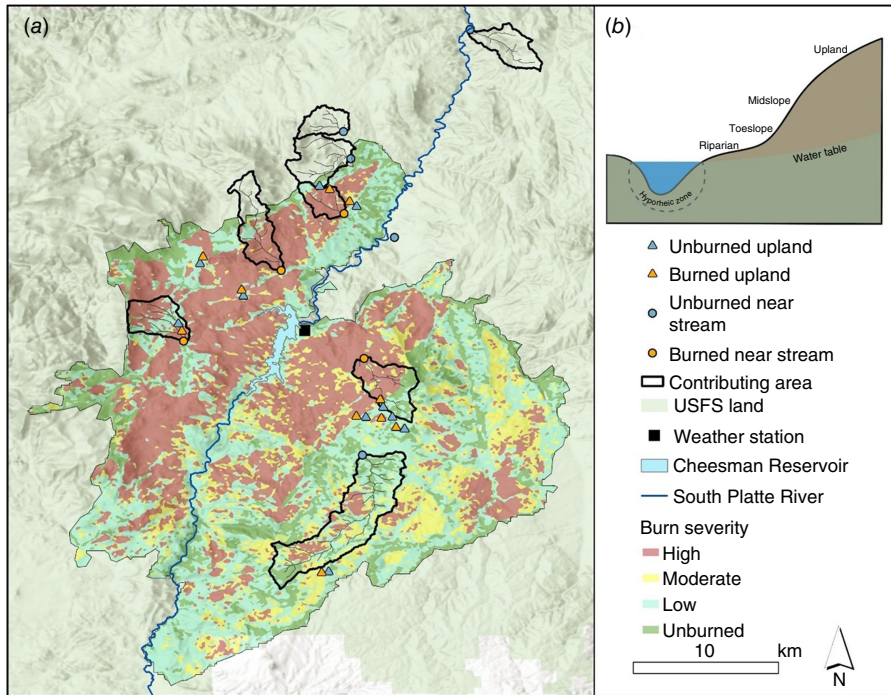


Fig. 1. (a) Sampling locations in watersheds within and adjacent to the 2002 Hayman fire, Colorado, USA. Triangles mark upland sites ($n = 20$). Circles mark near-stream networks, each of which contained six sites (i.e. riparian, toeslope and midslope on both stream banks), shown here as single points due to their close proximity. Burned sites are orange and unburned sites are blue. The Cheesman weather station is denoted by a black square (WRCC 2021). (b) Conceptual diagram of the four topographic positions along a hillslope used to structure site placement and represent landscape transitions from riparian to upland environments. USFS, United States Forest Service.

nutrient pulses (Rhoades *et al.* 2025a) and transient soil water repellency (Moody and Ebel 2012; Hallema *et al.* 2017; Williams *et al.* 2022) can enhance nutrient export after fire, these effects typically persist for less than 6 years (Debano 2000; Moody and Martin 2001; Williams *et al.* 2022). In contrast, our study evaluated patterns nearly two decades post-fire. Vegetation loss can alter hydrology over longer timescales, but these effects are often complex. For example, streamflow might increase from reduced evapotranspiration or streamflow could decrease due to reduced snow accumulation (Bart and Tague 2017; Kampf *et al.* 2022; McGrath *et al.* 2023). While such hydrologic changes may influence nutrient transport, this study focuses on the biogeochemical processes that sustain elevated NO_3^- export nearly two decades after fire.

In the spring of 2019, we established 68 sampling sites that were distributed along hillslopes spanning from uplands to near-stream riparian zones (Fig. 1b). Sampling was organized into two networks: near-stream and upland. Near-stream networks (Fig. 1a, circles) consisted of three discrete topographic positions within 10 m of the stream bank: (1) *riparian* – flat terrain within 1 m of the stream; (2) *toeslope* – the slope break between the riparian zone and hillslope; and (3) *midslope* – on the lower hillslope but still within 10 m of the stream. Each watershed included sites on both left and right banks, resulting in two riparian, two toeslope and two midslope sites per watershed. Across four burned and four unburned watersheds, this design produced 48 near-stream sites. Upland transects (Fig. 1a, triangles) were independent of stream proximity and spanned fire severity ecotones. Each of the 10 upland transects included one unburned and one severely burned site

approximately 500 m apart, totaling 20 upland sites. Together, the 48 near-stream and 20 upland sites allowed us to compare burned and unburned conditions across a continuum of topographic positions. These positions were selected to capture gradients in soil properties and vegetation composition that influence terrestrial N transport to streams (Fig. 1b). Wildfire severity was high to moderate (Eidenshink *et al.* 2009) at all burned sites though the extent and severity of fire in the upstream contributing areas varied (Rhea *et al.* 2022).

Field sampling and laboratory analyses

We measured total carbon (C) and N in the organic (O) and upper mineral soil (A) horizons to assess the lasting impacts of fire on soil C and N pools and as an index of post-fire substrate quality. The O horizon (i.e. litter + duff) was sampled from 0.1 m² quadrats, except in burned upland sites where there was no O horizon to sample. At each site, three mineral soil field replicates were collected within ~5 lateral meters from center using a bulb corer (11 cm depth, 7 cm diameter). Soil from each core was passed through a 2 mm sieve to remove coarse fragments. Laboratory analyses were conducted separately on each field replicate and results were then averaged to represent soil conditions for that site (e.g. one average of three field replicates for the riparian position on stream right in Brush watershed). Sub-samples from each horizon were dried for 24 h (at 105°C for A horizon, 65°C for O horizon), ground on a roller, and analyzed for total soil C and N by combustion reduction and infrared detection (CN 802, Velp Scientifica, Deer Park, NY). C and N stocks were calculated for the O and A horizons using total C and N

content, bulk density and sampling depth. Bulk density samples were collected with steel bulk density rings (7 cm depth, 8 cm diameter) driven into undisturbed mineral soils. Samples were oven-dried at 105°C for 24 h, and bulk density was calculated as dry mass divided by corer volume (g/cm^3).

We measured concentrations and microbially mediated production rates of plant-available N forms (NO_3^- and NH_4^+) in burned and unburned mineral soils. Again, three mineral soil field replicates were collected with a bulb corer (11 cm depth, 7 cm diameter) at each topographic position and stored on ice until processing. Fresh soils were passed through a 2 mm mesh sieve, and a 20 g subsample was extracted with 100 mL of 2 M potassium chloride (KCl), shaken for 60 min, filtered and analyzed for NO_3^- and NH_4^+ using spectroscopy (Lachat QuikChem AutoAnalyzer FIA + 800 Series, Loveland, CO). A 10 g subsample was oven dried at 105°C for 24 h to calculate gravimetric moisture content. A 50 g sub-sample was placed in a loosely capped plastic cup and incubated for 14 days at 20°C (Binkley and Hart 1989). Incubating samples were rewetted with deionized (DI) water periodically to maintain a moisture content of approximately 60% of field capacity. Field capacity was determined by saturating soil samples on a funnel, allowing them to drain under gravity for 24 h at room temperature and weighing the moisture retained after free drainage. After 14 days, subsamples of the incubated soils were extracted and analyzed as described above. Net mineralization was calculated as the difference in the sum of NO_3^- and NH_4^+ in initial and incubated soils and net nitrification as the change in NO_3^- (Hart *et al.* 1994). Negative mineralization rates indicate that soil microbes often immobilize all mineralized inorganic N.

We used *in situ* ion exchange resins (IER) to measure the amount of NO_3^- and NH_4^+ percolating within the top 5 cm of mineral soil (Binkley and Matson 1983). Two IER bags were installed at each of the three field replicate locations at each site (Fig. 1b). We deployed IER bags from May 2019 to October 2019 and October 2019 to May 2020 to characterize movement associated with summer rains and spring snowmelt, respectively. At the end of each deployment period, we extracted resins with 100 mL of 2 M KCl, shook samples for 60 min, filtered and analyzed the samples for NO_3^- and NH_4^+ concentrations as described above. In four of the eight watersheds, we also sampled root-zone soil water using 30 cm porous cup, tension lysimeters (Soil Moisture Corp, Goleta, CA). In each watershed, three lysimeters were installed at both riparian and toeslope positions and one lysimeter at each midslope position on both stream left and right. All lysimeters were located within 10 m of the stream. Lysimeters were not installed in the upland sites since shallow soil water was absent. In total, 56 lysimeters were spread across two burned and two unburned watersheds. We sampled leachate chemistry with a hand pump twice in May and monthly from June to September, as soil water availability permitted. The hand pump was purged with DI water and a sample rinse before each sample collection.

While post-fire stream water responses are well documented (Smith *et al.* 2011; Rust *et al.* 2018), the impacts on shallow groundwater remain less studied, despite their relevance for baseflow water chemistry and long-term nutrient retention. Only a few studies (e.g. Mansilha *et al.* 2020) have explored post-fire groundwater dynamics, underscoring the novelty of our multi-depth groundwater observations. We measured both sub-surface and surface water chemistry in two burned and two unburned watersheds, 1–2 times per month. The specific stream sampling locations were selected to isolate severely burned or unburned contributing area and do not necessarily correspond to the tributary outlets. We instrumented each watershed with two shallow groundwater wells, and two in-channel nested piezometers. The groundwater wells were installed on both sides of the stream to a 100 cm depth. Nested piezometers were installed at 40 and 80 cm depths in the center of the stream channel. Sub-surface water was sampled from wells and piezometers using a peristaltic pump purged with DI water and a sample rinse before each sample collection. Grab samples were also collected from the stream during each site visit.

All water samples from lysimeters, wells, piezometers and streams were stored on ice in acid-washed high-density polyethylene (HDPE) plastic bottles and filtered through 0.45 μm filters (Millipore Durapore PVDF, Billerica, MA). NO_3^- and NH_4^+ concentrations were measured with ion chromatography (Dionex Corp., Sunnyvale, CA). Detection limits were 0.01 mg/L for both NO_3^- and NH_4^+ . Sub-detection limit concentrations were replaced by one-half the detection limit concentration (0.005 mg/L).

We recorded water levels every 15 min throughout the summer using TruTrack capacitance rods (Intech Instruments Ltd. New Zealand) installed in all streams, wells and piezometers. Water level data were averaged by day and converted to station-specific z scores for comparison between stations. In addition, manual water level measurements were recorded biweekly to validate continuously recorded water levels.

Substrate and vegetative cover were measured within 1 m² quadrats located upstream of the middle transect at each landscape position (Fig. 1b). The percent cover of bare mineral soil was visually estimated, and vegetation was differentiated into forb, graminoid and shrub functional groups. We also recorded the tree species and whether each tree was alive or dead in a variable radius plot using a basal area gauge with a factor of 10.

Estimating vegetation productivity and N demand

We extracted remotely sensed estimates of terrestrial net primary productivity (NPP) from 1986 to 2021 for the 30-m pixel nearest to each field site using Google Earth Engine. These NPP estimates were partitioned by functional type (e.g. tree, shrub, herbaceous) based on the following procedure. The Rangeland Analysis Platform's fractional cover estimates by plant functional type (Jones *et al.* 2018; Allred *et al.*

2021) were used to disaggregate 30-m mixed pixel normalized difference vegetation index (NDVI) (Landsat) to functional type NDVI. Functional type NDVI was then integrated into the MOD17 net primary productivity model (Running *et al.* 2004) that was adapted to Landsat (Robinson *et al.* 2018) to estimate NPP by trees, shrubs and herbaceous functional types weighted by their fractional cover in each 30-m pixel (Robinson *et al.* 2019; Jones *et al.* 2021).

We linked post-fire changes in productivity to nutrient acquisition using nutrient use efficiency (NUE), which reflects how effectively vegetation converts N into biomass. Kaye *et al.* (2005) calculated functional group-specific NUEs by measuring biomass production and nutrient concentrations across fire and harvesting treatments with differing overstory and understory conditions. To estimate vegetation N uptake, we divided tree NPP fractions by ponderosa pine NUEs (106–107 kg C/kg N) and divided shrub and herbaceous NPP by herbaceous NUEs (51–52 kg C/kg N) (Kaye *et al.* 2005). Trees, that dominate unburned sites, were about twice as efficient at converting N into biomass compared to herbaceous vegetation, which dominate burned sites. This pattern aligns with the broader understanding that conifers are N-conservative, cycling available N tightly, whereas herbaceous species are more N-extravagant and contribute to more leaky N cycling (Chapman *et al.* 2006).

Statistical analyses

At each topographic position, three replicate mineral soil samples were collected for KCl-extractions and N mineralization incubations and six replicate IER bags were installed in 2019. After outlier removal, field replicates were averaged by topographic position within each site. We used the Shapiro test to assess data normality and used non-parametric statistics for all non-normal data. We first ran analysis of variances (ANOVAs) to test for interaction effects between burn condition (e.g. burned or unburned) and topographic position (e.g. riparian, toeslope, midslope or upland). Then, we used the Wilcoxon rank sum test to compare soil and water chemistry and vegetation between burned and unburned sites within each topographic position. Finally, we evaluated differences among the topographic positions in burned and unburned landscapes using Kruskal Wallis test. All statistical analyses were conducted in R (R Development Core Team) and significance was determined at the $\alpha = 0.1$ level.

Results

Soil N pools and transformations

At the time of our sampling 17 years post-fire, there was no O horizon in the severely burned uplands, and the O horizon was less than half as thick in burned compared to unburned

near-stream sites (1.2 vs 3 cm). When averaged across topographic positions, total N and C concentrations in burned O horizons were roughly 25% of that in unburned O horizons but did not differ significantly in the A horizons (Table 1). Due to lower concentrations and depths, O horizon C and N stocks were 76 and 79% lower, respectively in burned compared to unburned sites when averaged across topographic positions, with up to 100% reductions in uplands that dominate the burn scar (Table 1). In contrast, C and N stocks in the top 10 cm of the A horizon were similar across burned and unburned sites (Table 1). When averaged across topographic positions, total (O + A) stocks were 12,363 kg C/ha and 327 kg N/ha lower in burned sites, with O horizons accounting for 72% of C and 91% of N differences (Table 1). C:N ratios were similar in burned and unburned soils, with an average of 28 in the O and 22 in the A horizon. C and N concentrations were generally an order of magnitude greater in O than A horizons, but C and N stocks were much lower in O compared to A horizons due to their lower bulk density.

Extractable NO_3^- was significantly higher in burned compared to unburned mineral soils, with the greatest differences observed in midslope positions (16.0 vs 4.2 mg/kg; Table 2). Conversely, extractable NH_4^+ was significantly lower in burned than unburned mineral soils, especially in toeslope positions (0.9 vs 1.7 mg/kg; Table 2). On average, NO_3^- -N comprised a greater proportion of extractable N in burned (66%) compared to unburned (38%) mineral soils.

Lysimeter sampling during spring snowmelt demonstrated that NO_3^- concentrations in the top 30 cm of soil solution were 3.6 times higher in burned (0.61 mg/L) than unburned (0.17 mg/L) sites (Supplementary Fig. S2). Concurrently, IER NO_3^- , the mobile N anion, was also significantly higher in burned than unburned midslopes, with NO_3^- -N being 2.5 times more abundant than NH_4^+ -N (Fig. 2). IER NH_4^+ was consistently greater in burned soils, particularly during snowmelt (Fig. 2b). In burned watersheds, IER- NO_3^- declined in the downslope direction from midslope to riparian positions, especially during snowmelt. During the drier summer monsoon season (June–September), lysimeter NO_3^- concentrations declined to 0.53 mg/L in burned sites and increased to 0.24 mg/L in unburned sites.

Net N mineralization and nitrification rates were consistently lower in burned compared to unburned mineral soils, but burn effect was only statistically significant in midslopes or when averaged across topographic positions due to high variability (Table 2). Negative net mineralization rates were frequently observed, particularly in burned sites. However, in samples with positive net mineralization, nitrification accounted for two-thirds of total mineralized inorganic N.

Sub-surface and stream N

In near-stream zones, shallow groundwater (i.e. 40–100 cm wells and piezometers) NO_3^- concentrations were significantly

Table 1. Total nitrogen (N) and carbon (C) concentrations (%) and stocks (kg/ha) in organic (O) and upper mineral soil (A) horizons (0-10 cm).

			Concentration (%)					Stocks (kg/ha)				
			Riparian	Toeslope	Midslope	Upland	Average	Riparian	Toeslope	Midslope	Upland	Average
Total N	O horizon	Unburned	0.99	0.95*	1.09**	1.02	1.01**	261	389**	553**	377**	394**
		Burned	0.82	0.76*	0.71**	–	0.77**	225	143**	38**	0**	96**
	A horizon	Unburned	0.13	0.15	0.16	0.12	0.14	1,252	1,429	1,562	1,541	1,458
		Burned	0.16	0.14	0.10	0.12	0.13	1,617	1,481	1,194	1,426	1,429
	Total	Unburned						1,513	1,818	2,115**	1,918	1,852*
	O + A	Burned						1,842	1,624	1,232**	1,426	1,525*
Total C	O horizon	Unburned	26	30	35**	25	29**	7,783	11,598**	17,155**	9,062**	11,262**
		Burned	19	24	20**	–	21**	4,585	4,213**	1,032**	0**	2,313**
	A horizon	Unburned	3.0	4.0	3.6	2.4	3.2	28,053	38,894	35,517	29,349	32,883
		Burned	3.1	3.5	2.0	2.2	2.7	32,272	35,742	25,103	25,703	29,469
	Total	Unburned						35,836	50,492	52,672**	38,411*	44,145**
	O + A	Burned						36,857	39,955	26,135**	25,703*	31,782**

68 samples were averaged within and across topographic positions. There was no O horizon to sample in burned uplands. Asterisks denote significant differences between burned and unburned soils within each topographic position and soil layer (**P* < 0.1 and ***P* < 0.05).

Table 2. Soil extractable nitrate (NO_3^-) and ammonium (NH_4^+) pools (mg/kg) from the top 10 cm of burned and unburned mineral soils.

Pools and processing rates	Fire effect	A horizon					Average
		Riparian	Toeslope	Midslope	Upland		
Extractable NO_3^- (mg/kg)	Unburned	3.1	3.3	4.2**	1.2	2.8**	
	Burned	2.6	9.5	16.0**	1.3	7.0**	
Extractable NH_4^+ (mg/kg)	Unburned	1.0	1.7*	1.1	1.6	1.3*	
	Burned	1.2	0.9*	0.7	1.3	1.1*	
Net mineralization (kg N/ha.day)	Unburned	0.05	0.10	0.09	0.03	0.06**	
	Burned	-0.02	-0.03	-0.08	0.02	-0.02**	
Net nitrification (kg N/ha.day)	Unburned	0.04	0.10	0.10*	0.09	0.08*	
	Burned	0.02	0.00	-0.06*	0.07	0.01*	

Net nitrogen (N) mineralization and net nitrification rates (kg N/ha.day) from 14-day aerobic laboratory incubations of mineral soils (0–10 cm). Negative transformations indicate that microbial uptake (e.g. immobilization) exceeds the production of inorganic N. 68 samples were averaged by topographic position and fire effect for this summary table. Asterisks denote significant differences between burned and unburned soils within each topographic position and soil layer (* $P < 0.1$ and ** $P < 0.05$).

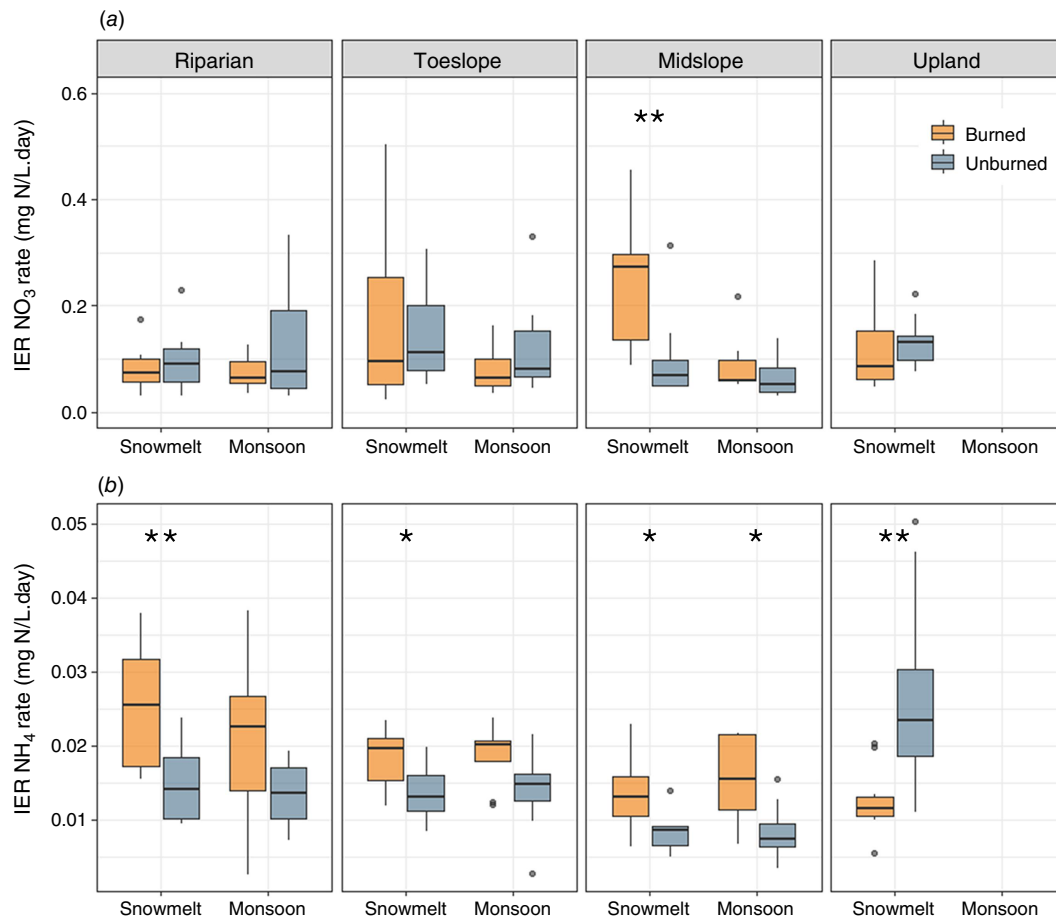


Fig. 2. Ion exchange resin (IER) (a) nitrate (NO_3^-) and (b) ammonium (NH_4^+) accumulation rates separated by summer monsoon and spring snowmelt seasons. This represents plant-available inorganic nitrogen (N) in the top 5 cm of mineral soil. Upslope positions only have winter data. The centerline of the boxplots denotes the median values, the upper and lower limits span the interquartile range, the whiskers include data within 1.5 times the interquartile range and the dots beyond the whiskers are outliers. Fire effect significance is denoted by * $P < 0.1$ and ** $P < 0.05$.

higher in burned (0.64–4.07 mg/L) compared to unburned (0.01–3.42 mg/L) sites (Fig. 3a, b). Stream NO_3^- concentrations were 10-times higher in burned (avg = 2.1, 0.67–4.25 mg/L) compared to unburned sites (avg = 0.21, 0.01–0.59 mg/L) across seasons (Fig. 3c) confirming that previously reported patterns of elevated NO_3^- in these burned streams (Rhoades et al. 2011, 2019) are still present at the time of this study. In unburned watersheds, stream NO_3^- was quite low throughout the sampling period and peaked in August (Fig. 3c). In burned watersheds, surface and sub-surface NO_3^- concentrations generally peaked during spring snowmelt (May–June) (Fig. 3). In the subset of four watersheds that were intensively monitored for water chemistry, stream NO_3^- concentrations did not monotonically decline through the summer and exhibited secondary peaks in August. However, long-term monitoring across a broader network of burned watersheds consistently shows that the highest post-fire stream NO_3^- concentrations occur during the spring peak discharge period (Rhoades et al. 2011, 2019). NH_4^+ concentrations ranged from 0.005 mg/L (i.e. below detection limit) to 0.75 mg/L across all sampling

locations and dates. On average, NO_3^- -N comprised a greater proportion of total dissolved N in burned streams (68%) compared to unburned streams (34%).

Vegetation composition, productivity and N demand

The unburned overstory was dominated by ponderosa pine and Douglas-fir, with average basal areas of 15 and 11 m^2/ha , respectively. The fire caused complete mortality of mature trees in our burned study sites, with no evidence of conifer regeneration to date. Quaking aspen was present in both burned and unburned near-stream environments, likely due to mesic conditions, with an average basal area of 15 m^2/ha . Despite high fire severity and complete overstory mortality, understory vegetation cover was generally greater in burned uplands. Graminoid (30% vs 12%), forb (4.5% vs 2.0%) and shrub (11% vs 5.2%) cover were 2–2.6 times higher in burned than in unburned sites, even though bare mineral soil also increased substantially (59% vs 2%) (Fig. 4). Graminoids

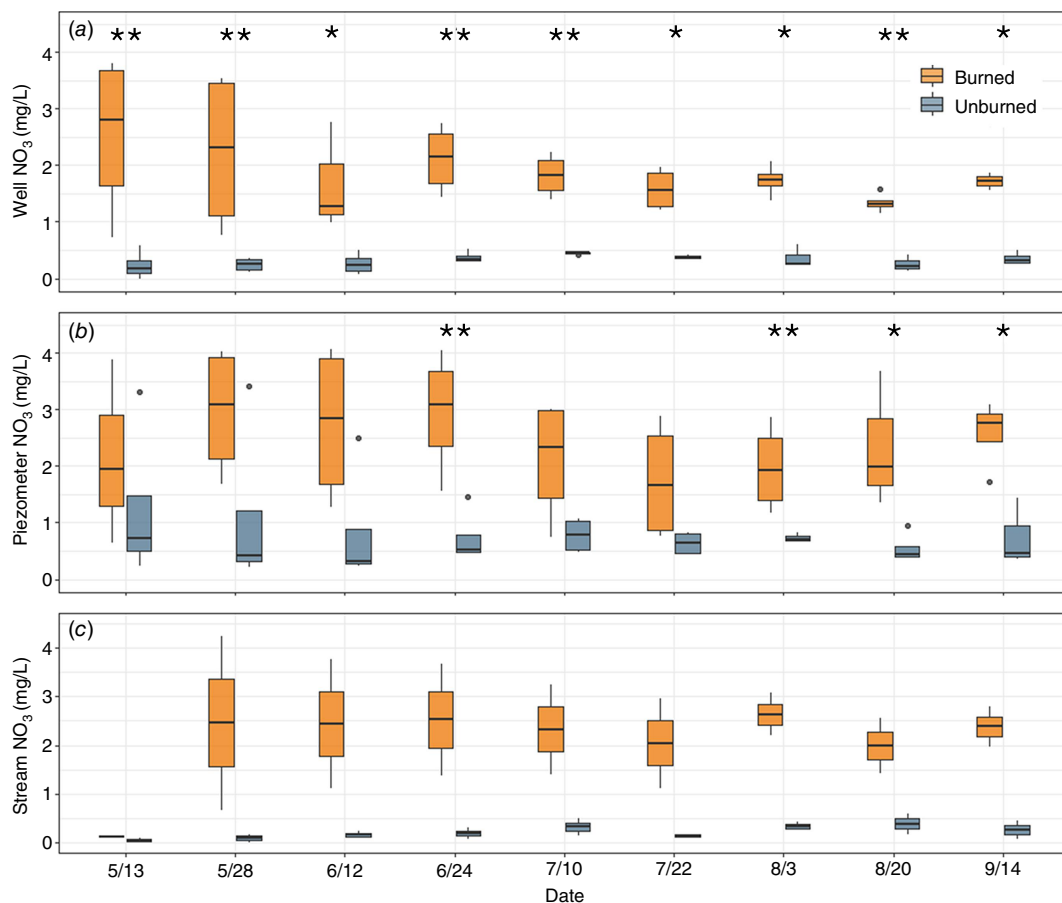


Fig. 3. Time series of nitrate (NO_3^-) concentrations in shallow groundwater from (a) riparian wells (1 m), (b) in-stream nested piezometers (40 and 80 cm), and (c) stream water from burned (orange) and unburned (blue) watersheds. The centerline of the boxplots denotes the median values, the upper and lower limits span the interquartile range, the whiskers include data within 1.5 times the interquartile range, and the dots beyond the whiskers are outliers. Fire effect significance is denoted by * $P < 0.1$ and ** $P < 0.05$.

were dominant, accounting for an average of 30% of vegetative cover in burned sites and 12% in unburned sites (Fig. 4).

Total estimated pre-fire NPP was similar at burned (4,035 kg C/ha.year) and unburned sites (4,046 kg C/ha.year) (Fig. 5) and aligns with reported values from other Western conifer forests (2,600–6,200 kg C/ha.year) (Turner *et al.* 2004, 2009; Kaye *et al.* 2005). However, the 2002 Hayman fire caused an immediate 64 and 77% reduction (Δ of 2,884 and 2,736 kg C/ha.year) in NPP in burned near-stream and upland sites, respectively (Table 3). By 2019, total NPP was

46 and 59% lower (Δ of 2,091 of and 2,111 kg C/ha.year) in burned near-stream and upland sites compared to pre-fire conditions (Table 3). On average, trees comprised 88% of NPP in unburned sites across all years (Fig. 5a). At our burned sites, trees accounted for 84% of NPP pre-fire but shifted to understory-dominance with shrubs and herbs comprising 90% of NPP 17 years after the fire (Fig. 5b).

Before the fire, shrubs and herbs accounted for 22–29% of total vegetation N uptake (Table 3). Post-fire, their contribution increased to 62–77% in 2003 and 92–97% in 2019.

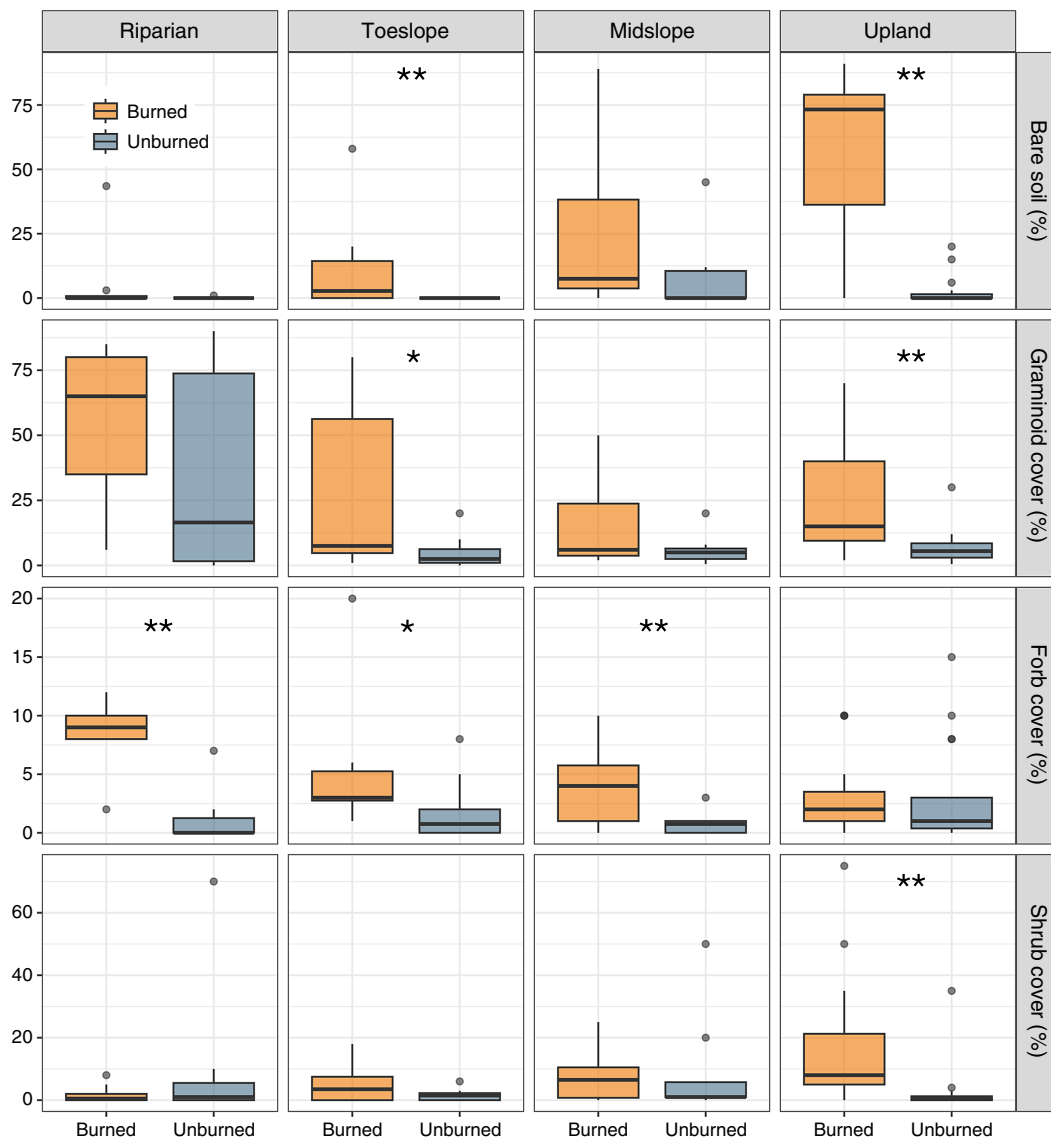


Fig. 4. Bare mineral soil and understory vegetation cover estimates by burn and topography factors. Surface (i.e. bare mineral soil) and vegetative (i.e. graminoid, forb and shrub) cover were measured independently and will not sum to 100%. The centerline of the boxplots denotes the median values, the upper and lower limits span the interquartile range, the whiskers include data within 1.5 times the interquartile range, and the dots beyond the whiskers are outliers. Fire effect significance is denoted by * $P < 0.1$ and ** $P < 0.05$.

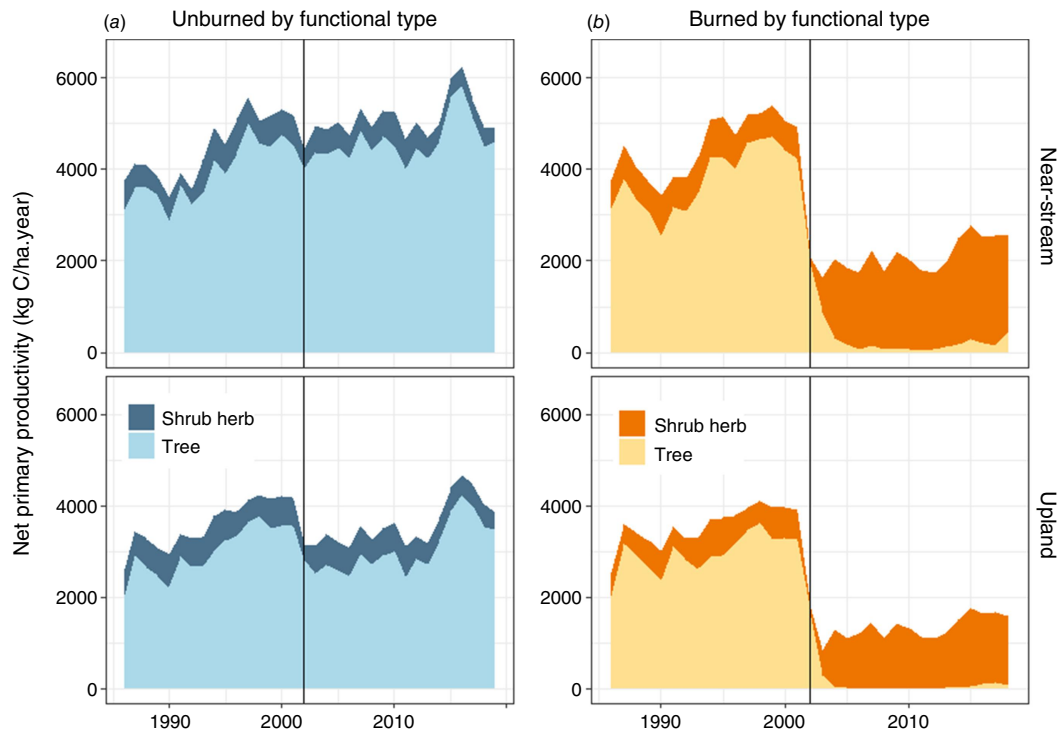


Fig. 5. Annual terrestrial net primary productivity (NPP) (kg C/ha.year) by functional type for (a) unburned and (b) burned sites. The upper panels represent near-stream sites and lower panels upland sites. NPP is partitioned by plant functional type which is illustrated with color shading. The vertical black line represents the year of the 2002 Hayman Fire.

Table 3. Estimated net primary productivity (NPP), nitrogen use efficiency (NUE) and vegetation nitrogen (N) uptake summarized by burn condition, landscape position, functional type and year.

Condition	Position	Component	NPP (kg C/ha.year)			NUE (kg C/kg N)	N uptake (kg N/ha.year)		
			Pre-fire (1986–2001)	Post-fire (2003)	Post-fire (2019)		Pre-fire (1986–2001)	Post-fire (2003)	Post-fire (2019)
Unburned	Near-stream	Shrub herb	561	588	299	52	11	11	6
		Tree	3,919	4,357	4,607	107	37	41	43
		Total	4,479	4,944	4,906		48	52	49
	Upland	Shrub herb	600	610	374	52	12	12	7
		Tree	3,013	2,520	3,476	107	28	24	32
		Total	3,613	3,130	3,850		40	36	39
Burned	Near-stream	Shrub herb	712	714	2,117	51	14	14	42
		Tree	3,795	909	300	106	36	9	3
		Total	4,507	1,623	2,416		50	23	45
	Upland	Shrub herb	592	514	1,369	51	12	10	27
		Tree	2,972	313	85	106	28	3	1
		Total	3,564	828	1,453		40	13	28

NUE values were calculated from measurements in control and treated (i.e. thinned and burned) ponderosa pine forests in Arizona, USA (Kaye et al. 2005). Control sites with higher tree density and basal area from Kaye et al. (2005) were matched to unburned sites in our study whereas treated plots with lower tree density and basal area were matched to burned plots.

At the time of our field sampling in 2019, estimated vegetation N uptake in burned near-stream sites (45 kg N/ha.year) was ~10% lower than in unburned near-stream sites (49 kg N/ha.year) and pre-fire conditions (50 kg N/ha.year). In upland areas, 2019 estimates showed a larger ~30% reduction in burned sites (28 kg N/ha.year) compared to unburned (39 kg N/ha.year) and pre-fire (40 kg N/ha.year) estimates. Furthermore, an inverse relationship between annual vegetation NPP and minimum summer NO_3^- concentrations in both shallow groundwater and streams indicates that sites with lower NPP tend to have higher residual NO_3^- levels (Fig. 6).

Discussion

Indices of soil N availability

Inorganic N availability was consistently higher in burned than unburned watersheds throughout the shallow subsurface (0–100 cm). Mineral soil extractable NO_3^- was 2.5-times greater in burned soils across hillslope positions and NO_3^- -N comprised a greater proportion of extractable inorganic N in burned soils (66% vs 38%; Table 2). Similarly, IER – NO_3^- was twice as high in burned compared to unburned midslope positions (0.16 vs 0.08 mg NO_3^- /L.day)

across seasons (Fig. 2a). Peak soil solution NO_3^- during snowmelt was 3.6-times higher in burned sites (0.61 vs 0.17 mg/L). During the summer monsoon, those concentrations declined in burned sites (0.53 mg/L) but remained elevated relative to unburned sites (0.24 mg/L), reflecting persistent post-fire enrichment. These surface patterns were mirrored at depth, providing novel evidence of post-fire N enrichment extending into deeper subsurface zones (30–100 cm). Subsurface NO_3^- concentrations were 3.6-, 2.7- and 5.8-times higher in burned compared to unburned lysimeters, piezometers and wells, respectively (Supplementary Fig. S2). Together, these findings demonstrate that fire significantly enhances and sustains inorganic N availability, consistent with other studies demonstrating increased NO_3^- mobilization after fire (Hanan *et al.* 2016a; Gustine *et al.* 2022).

Despite elevated inorganic N availability, net N mineralization rates were low across all sites (–0.1 to 0.1 kg N/ha.day), with slightly lower rates in burned mineral soils (Table 2). Including forest floor contributions could have roughly doubled our net mineralization estimates, consistent with findings that O horizons account for about half of total net mineralization in undisturbed forests in this region (Stump and Binkley 1992). This would likely have disproportionately increased mineralization in unburned sites with more developed forest floors. Contrary to our hypothesis and to findings from other studies (Wan *et al.* 2001; Dove *et al.* 2020), net N mineralization was not elevated in burned mineral soils (Table 2). Annualized N mineralization rates in mineral soils were notably smaller than other major ecosystem fluxes (Table 4). This disparity was most pronounced in burned watersheds, where annualized mineralization was negative and orders of magnitude lower than vegetation N uptake. Thus, we conclude that microbial production of inorganic N does not account for elevated N observed in soils, shallow subsurface flow and streams in burned watersheds.

Vegetation productivity and N demand

Vegetation productivity remained suppressed for 17 years after the Hayman Fire due to fire-induced mortality and slow recovery. At the time of sampling in 2019, total NPP was 46–59% lower than pre-fire conditions and 51–62% lower compared to unburned sites (Table 3). There was also a dramatic shift from tree-dominated NPP before the fire (83% of total NPP in uplands) to herbaceous-dominated NPP post-fire (95%). Post-fire herbaceous cover rapidly exceeded pre-fire levels (Fornwalt *et al.* 2018), and graminoid, forb and shrub cover increased 3.5-fold in burned uplands. However, total vegetative cover remained low (~43%). The limited understory recovery was insufficient to offset the substantial loss of tree-associated NPP. This contrasts sharply with other fire-affected systems that experienced faster tree regeneration. For example, following

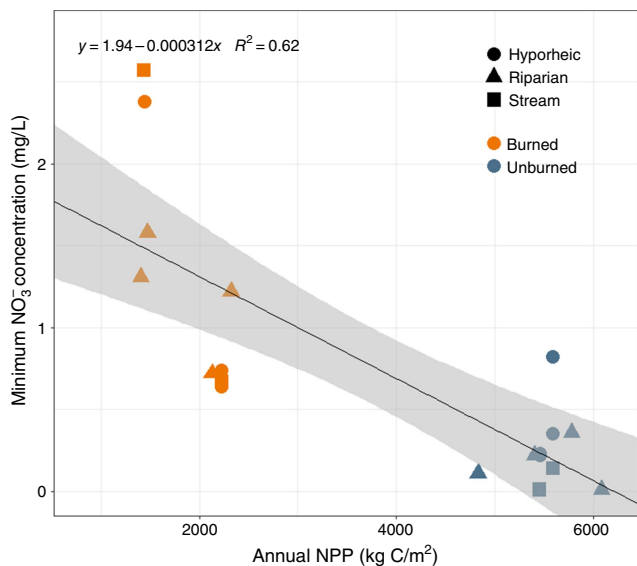


Fig. 6. Inverse relationship between remotely-sensed annual net primary productivity (NPP) and minimum summer nitrate (NO_3^-) concentration in near-stream water sources across multiple burned (orange) and unburned (blue) watersheds. Minimum NO_3^- concentrations were measured during the summer low-flow period in streams (squares), riparian groundwater wells (triangles) and hyporheic-zone piezometers (circles). NPP represents total annual productivity (tree and herbaceous) in near-stream areas for the same year as NO_3^- sampling. This comparison highlights consistent patterns across catchments and water sources, suggesting lower NPP is associated with elevated summertime NO_3^- availability.

Table 4. Major nitrogen (N) fluxes (kg N/ha.year) in burned and unburned watersheds based on study measurements and literature values.

	N fluxes (kg N/ha.year)						
	Unburn			Burn			
	Min	Mean	Max	Min	Mean	Max	
N deposition (Heindel <i>et al.</i> 2022)	2.5	3.5	4.4	=	2.5	3.5	4.4
A horizon net mineralization (Table 2)	5	11	18	>	-14	-4	4
Vegetation N uptake (Table 3)	39	44	49	>	28	37	45
Denitrification (Barton <i>et al.</i> 1999)		1		=		1	
Watershed TDN export (Rhoades <i>et al.</i> 2019)		0.12		<		0.65	

These values do not represent a closed N budget as they combine our measurements with locally relevant peer-reviewed literature. Daily N mineralization rates (Table 2) were rescaled to annual estimates assuming six snow-free months from May to October. A, upper mineral soil; TDN, total dissolved N.

the 1988 Yellowstone fires, extensive lodgepole pine regeneration resulted in trees contributing 79% of total productivity (4,900 kg C/ha.year tree vs 1,300 kg C/ha.year herbaceous) just 15 years post-fire (Turner *et al.* 2009). In comparison, total upland NPP at Hayman (1,453 kg C/ha.year) remained much lower 17 years post-fire than values reported after Yellowstone (6,200 kg C/ha.year), underscoring the slow pace of vegetation recovery in this system – a trend observed following more recent wildfires across Colorado and the Western USA (Stevens-Rumann *et al.* 2018; Davis *et al.* 2019).

Post-fire shifts in vegetation composition suggest altered N use efficiency, prompting closer examination of changes in vegetation N uptake. Estimated vegetation N uptake was lower in burned compared to unburned sites, with a 28% reduction in uplands and an 8% reduction in near-stream environments (Table 3). However, the post-fire decline in N uptake was smaller than the NPP reductions due to increased dominance of herbaceous vegetation following the fire. Herbaceous species require more N per unit of assimilated C than coniferous trees (Kaye *et al.* 2005; Chapman *et al.* 2006), which partially offsets the reduction in productivity. Nevertheless, these shifts were insufficient to restore N demand to pre-fire or unburned levels. Overall, remotely sensed estimates demonstrate a substantial, long-term reduction in vegetation N demand after the Hayman fire, particularly in uplands which comprise a majority of the burned landscape. Our findings demonstrate that reduced vegetation N uptake is the primary driver of elevated post-fire N export, representing the largest change in ecosystem N fluxes (Table 4).

NO₃⁻ transport

NO₃⁻ dynamics shift from biotic limitation in unburned watersheds to episodic loss in burned watersheds with reduced vegetation demand. In unburned watersheds, which are typically N-limited, NO₃⁻ concentrations remained low throughout our sampling period (Fig. 3c), consistent with source limitation where high biotic demand restricts N export (Godsey *et al.* 2009; Basu *et al.* 2011; Shogren *et al.* 2021). In contrast, burned watersheds exhibited elevated NO₃⁻ concentrations,

with distinct peaks during spring snowmelt and summer monsoons (Fig. 3c). These increases in NO₃⁻ with streamflow align with other post-fire studies (Bladon *et al.* 2008; Mast *et al.* 2016) and long-term monitoring at these burned sites (Rhoades *et al.* 2019). This pattern reflects transport-limited conditions, where NO₃⁻ supply exceeds biotic demand and is episodically flushed during periods of hydrologic connectivity (Basu *et al.* 2011; Creed *et al.* 2015).

Multiple lines of evidence suggest that this post-fire export is sustained by persistent subsurface NO₃⁻ availability. Lysimeter and IER measurements show elevated NO₃⁻ availability in the rooting zone of burned sites during both spring snowmelt and summer monsoons (Fig. 2, Supplementary Fig. S2), positioning mobile NO₃⁻ in hydrologically active zones. Reduced vegetation uptake further amplifies this effect. Minimum summer NO₃⁻ concentrations were inversely related to NPP across our sites, suggesting that lower biotic demand facilitates continued accumulation and availability of NO₃⁻ for episodic transport to streams.

Notably, elevated stream NO₃⁻ concentrations in burned watersheds persist even during baseflow (October–January) (Rhoades *et al.* 2019), likely reflecting contributions from NO₃⁻-enriched groundwater (Fig. 3). This legacy NO₃⁻ may originate from mineralization in earlier post-fire years, gradually leaching into shallow groundwater over time during periods of hydrologic connection.

Together, our findings show that long-term stream NO₃⁻ export is sustained by reduced vegetation uptake, persistent subsurface NO₃⁻ availability, episodic flushing during periods of hydrologic connectivity and groundwater contributions. Although pre-fire stream NO₃⁻ concentrations did not differ between burned and unburned sites (Rhoades *et al.* 2011), the elevated post-fire concentrations and seasonal dynamics described here have persisted for nearly two decades (Rhoades *et al.* 2019). This suggests that post-fire biogeochemical shifts can have long-lasting effects, extending well beyond the immediate disturbance window typically studied.

Implications for post-fire watershed restoration

Lower than expected post-fire tree regeneration has been widely observed, particularly where severe wildfires are

followed by hot, dry conditions (Stevens-Rumann *et al.* 2018; Davis *et al.* 2019). This has generated interest in active reforestation across western North America (U.S. Department of Agriculture 2023). However, reforestation capacity (e.g. seed supply, nursery production and planting labor) lags far behind current and projected needs (Fargione *et al.* 2021), forcing managers to prioritize planting efforts. Most projects focus on planting upland areas with low regeneration potential (Chambers *et al.* 2016; Stevens-Rumann and Morgan 2019; Rhoades *et al.* 2025b), but our results suggest that planting within near-stream areas may have disproportionate benefits for stream water quality and other ecosystem resources (Erdozain *et al.* 2021).

In the Hayman burn, upland soils exhibited the highest net nitrification rates and the lowest soil NO_3^- concentrations across hillslope positions (Table 2, Fig. 2). Vegetation N uptake was also lowest in burned uplands (Fig. 5). Together, these conditions contributed to substantial NO_3^- losses via leaching and subsurface transport. Water and nutrients moving downslope from uplands often accumulate in topographically convergent areas such as swales or ephemeral channels. Although these zones are not classified as riparian, they can provide similar hydrologic and biogeochemical functions. Where post-fire vegetation recovery is limited, convergent hillslopes act as concentrated sources of downgradient NO_3^- (Rhea *et al.* 2022). Prioritizing reforestation in such locations has the potential to retain nutrients in upland landscapes. Furthermore, the relatively high soil moisture in these zones should favor seedling survival and growth.

The decrease in soil NO_3^- in riparian zones (Table 2, Fig. 2) likely reflects increased N uptake by near-stream vegetation (Table 3) and potentially gaseous N losses from anoxic soils via denitrification (Hill 1996). Vegetation N uptake was 1.6 times higher in near-stream zones than uplands, likely resulting from rapid regrowth of sprouting riparian species as opposed to sparse regeneration observed in the uplands. Our findings align with research conducted elsewhere that has documented the role of vegetation in mitigating watershed N export after severe fire (Smithwick *et al.* 2009), beetle outbreaks (Rhoades *et al.* 2013) and timber harvesting (Bormann and Likens 1979).

Our results suggest that increasing vegetation in floodplains and riparian zones may benefit post-fire water quality. Planting herbaceous and shrub species in low-gradient, unconfined meadows has been shown to enhance N retention (Mitsch *et al.* 2005; Postila and Heiderscheidt 2020), especially when paired with in-stream structures (e.g. post assisted log structures or beaver dam analogs) that improve hydrologic connectivity (Silverman *et al.* 2019). Herbaceous, shrub and tree plantings that extend away from the stream channels mimic vegetated buffer strips which are a well-established approach for reducing nutrient runoff and improving water quality in agricultural areas (Mayer *et al.* 2007; Dosskey *et al.* 2010). In combination

with upland reforestation, restoring convergent hillslopes, floodplains and riparian zones has the potential to focus post-fire interventions on reducing NO_3^- losses and supporting watershed recovery.

Conclusions

Elevated post-fire stream NO_3^- can persist for years to decades (Smith *et al.* 2011; Rust *et al.* 2018; Rhoades *et al.* 2019). This study investigated the mechanisms behind long-term NO_3^- export following severe wildfire, emphasizing the balance between soil N availability and vegetation demand. Inorganic soil N measured in KCl and resin extracts, soil water and shallow groundwater was generally elevated in burned compared to unburned sites (Figs 2, 3, Tables 1, 2). Conversely, we found no evidence that inorganic N supplied by mineralization was higher in burned mineral soils. Because much of the NO_3^- and NH_4^+ in these forests originates in the O horizon, and that layer is reduced or absent in severely burned areas, overall N production in burned sites is likely lower than in unburned sites.

Forest recovery over the 17 years since the Hayman fire has been limited. Remote sensing estimates indicate that vegetation productivity and N demand are 51–62 and 8–28% lower in burned compared to unburned areas, respectively. The greatest decrease in vegetation occurred in the upland areas that dominate the burn scar, where N supply in soils exceeded vegetation N demand. It appears that this imbalance is the primary driver of persistent subsurface transport of NO_3^- from burned uplands to streams.

The link between vegetation recovery and watershed N retention has important implications for land managers confronting poor post-fire regeneration, an increasingly common concern in western North America. Reforestation efforts that enhance tree cover in uplands while promoting recovery of riparian vegetation have the potential to improve watershed-scale N retention following severe wildfires.

Supplementary material

Supplementary material is available online.

References

- Allred BW, Bestelmeyer BT, Boyd CS, Brown C, Davies KW, Duniway MC, Ellsworth LM, Erickson TA, Fuhlendorf SD, Griffiths T V, Jansen V, Jones MO, Karl J, Knight A, Maestas JD, Maynard JJ, McCord SE, Naugle DE, Starns HD, Twidwell D, Uden DR (2021) Improving Landsat predictions of rangeland fractional cover with multitask learning and uncertainty. *Methods in Ecology and Evolution* 12, 841–849. doi:10.1111/2041-210x.13564
- Bart RR, Tague CL (2017) The impact of wildfire on baseflow recession rates in California. *Hydrological Processes* 31(8), 1662–1673. doi:10.1002/hyp.11141
- Barton L, McLay CDA, Schipper LA, Smith CT (1999) Annual denitrification rates in agricultural and forest soils: a review.

- Australian Journal of Soil Research* 37(6), 1073–1093. doi:10.1071/SR99009
- Basu NB, Thompson SE, Rao PSC (2011) Hydrologic and biogeochemical functioning of intensively managed catchments: a synthesis of top-down analyses. *Water Resources Research* 47(10), 1–12. doi:10.1029/2011WR010800
- Bauhus J, Khanna PK, Raison RJ (1993) The effect of fire on carbon and nitrogen mineralization and nitrification in an Australian forest soil. *Australian Journal of Soil Research* 31(5), 621–639. doi:10.1071/SR9930621
- Biederman JA, Meixner T, Harpold AA, Reed DE, Gutmann ED, Gaun JA, Brooks PD (2016) Riparian zones attenuate nitrogen loss following bark beetle-induced lodgepole pine mortality. *Journal of Geophysical Research: Biogeosciences* 121(3), 933–948. doi:10.1002/2015JG003284
- Binkley D, Hart SC (1989) The components of nitrogen availability assessments in forest soils. In 'Advances in Soil Science', 10th edn. (Ed. BA Stewart) pp. 57–112. (Springer-Verlag)
- Binkley D, Matson P (1983) Ion exchange resin bag method for assessing forest soil nitrogen availability. *Soil Science Society of America Journal* 47(5), 1050–1052. doi:10.2136/sssaj1983.03615995004700050045x
- Bladon KD, Silins U, Wagner MJ, Stone M, Emelko MB, Mendoza CA, Devito KJ, Boon S (2008) Wildfire impacts on nitrogen concentration and production from headwater streams in southern Alberta's Rocky Mountains. *Canadian Journal of Forest Research* 38(9), 2359–2371. doi:10.1139/X08-071
- Bormann FH, Likens GE (1979) Catastrophic disturbance and the steady-state in northern hardwood forests. *American Scientist* 67(6), 660–669.
- Chambers ME, Fornwalt PJ, Malone SL, Battaglia MA (2016) Patterns of conifer regeneration following high severity wildfire in ponderosa pine – dominated forests of the Colorado Front Range. *Forest Ecology and Management* 378, 57–67. doi:10.1016/j.foreco.2016.07.001
- Chapin FS, Mooney HA, Matson PA (2011) 'Principles of terrestrial ecosystem ecology.' 2nd edn. (Springer: New York, NY, USA)
- Chapman SK, Langley JA, Hart SC, Koch GW (2006) Plants actively control nitrogen cycling: uncorking the microbial bottleneck. *New Phytologist* 169(1), 27–34. doi:10.1111/j.1469-8137.2005.01571.x
- Covington WW, Sackett SS (1992) Soil mineral nitrogen changes following prescribed burning in ponderosa pine. *Forest Ecology and Management* 54(1–4), 175–191. doi:10.1016/0378-1127(92)90011-W
- Creed IF, McKnight DM, Pellerin BA, Green MB, Bergamaschi BA, Aiken GR, Burns DA, Findlay SEG, Shanley JB, Striegl RG, Aulenbach BT, Clow DW, Laudon H, McGlynn BL, McGuire KJ, Smith RA, Stackpoole SM (2015) The river as a chemostat: fresh perspectives on dissolved organic matter flowing down the river continuum. *Canadian Journal of Fisheries and Aquatic Sciences* 72(8), 1272–1285. doi:10.1139/cjfas-2014-0400
- Davis KT, Dobrowski SZ, Higuera PE, Holden ZA, Veblen TT, Rother MT, Parks SA, Sala A, Maneta MP (2019) Wildfires and climate change push low-elevation forests across a critical climate threshold for tree regeneration. *Proceedings of the National Academy of Sciences of the United States of America* 116(13), 6193–6198. doi:10.1073/pnas.1815107116
- Debano LF (2000) The role of fire and soil heating on water repellency in wildland environments: a review. *Journal of Hydrology* 231–232, 195–206. doi:10.1016/S0022-1694(00)00194-3
- Dosskey MG, Vidon P, Gurwick NP, Allan CJ, Duval TP, Lowrance R (2010) The role of riparian vegetation in protecting and improving chemical water quality in streams. *Journal of the American Water Resources Association* 46(2), 261–277. doi:10.1111/j.1752-1688.2010.00419.x
- Dove NC, Safford HD, Bohlman GN, Estes BL, Hart SC (2020) High-severity wildfire leads to multi-decadal impacts on soil biogeochemistry in mixed-conifer forests. *Ecological Applications* 30(4), e02072. doi:10.1002/eap.2072
- Dunnette PV, Higuera PE, Mclauchlan KK, Derr KM, Briles CE, Keefe MH (2014) Biogeochemical impacts of wildfires over four millennia in a Rocky Mountain subalpine watershed. *New Phytologist* 203(3), 900–912. doi:10.1111/nph.12828
- Dwire KA, Kauffman JB (2003) Fire and riparian ecosystems in landscapes of the western USA. *Forest Ecology and Management* 178(1–2), 61–74. doi:10.1016/S0378-1127(03)00053-7
- Eidenshink J, Schwind B, Brewer K, Zhu Z-L, Quayle B, Howard S (2009) A project for monitoring trends in burn severity. *Fire Ecology* 3(1), 3–21. doi:10.4996/fireecology.0301003
- Erdozain M, Kidd KA, Emilson EJS, Capell SS, Kreutzweiser DP, Gray MA (2021) Forest management impacts on stream integrity at varying intensities and spatial scales: do abiotic effects accumulate spatially? *Science of The Total Environment* 753, 141968. doi:10.1016/j.scitotenv.2020.141968
- Fargione J, Haase DL, Burney OT, Kildisheva OA, Edge G, Cook-Patton SC, Chapman T, Rempel A, Hurteau MD, Davis KT, Dobrowski S, Enebak S, De La Torre R, Bhuta AAR, Cubbage F, Kittler B, Zhang D, Guldin RW (2021) Challenges to the reforestation pipeline in the United States. *Frontiers in Forests and Global Change* 4, 629198. doi:10.3389/ffgc.2021.629198
- Fornwalt PJ, Kaufmann MR (2014) Understorey plant community dynamics following a large, mixed severity wildfire in a *Pinus ponderosa-Pseudotsuga menziesii* forest, Colorado, USA. *Journal of Vegetation Science* 25(3), 805–818. doi:10.1111/jvs.12128
- Fornwalt PJ, Stevens-Rumann CS, Collins BJ (2018) Overstorey structure and surface cover dynamics in the decade following the Hayman fire, Colorado. *Forests* 9(3), 1–17. doi:10.3390/f9030152
- Godsey SE, Kirchner JW, Clow DW (2009) Concentration–discharge relationships reflect chemostatic characteristics of US catchments. *Hydrological Processes* 23, 1844–1864. doi:10.1002/hyp.7315
- Gustine RN, Hanan EJ, Robichaud PR, Elliot WJ (2022) From burned slopes to streams: how wildfire affects nitrogen cycling and retention in forests and fire-prone watersheds. *Biogeochemistry* 157(1), 51–68. doi:10.1007/s10533-021-00861-0
- Hallema DW, Sun G, Bladon KD, Norman SP, Caldwell P V, Liu Y, McNulty SG (2017) Regional patterns of postwildfire streamflow response in the western United States: the importance of scale-specific connectivity. *Hydrological Processes* 31(14), 2582–2598. doi:10.1002/hyp.11208
- Hanan EJ, D'Antonio CM, Roberts DA, Schimel JP (2016a) Factors regulating nitrogen retention during the early stages of recovery from fire in coastal chaparral ecosystems. *Ecosystems* 19(5), 910–926. doi:10.1007/s10021-016-9975-0
- Hanan EJ, Schimel JP, Dowdy K, D'Antonio CM (2016b) Effects of substrate supply, pH, and char on net nitrogen mineralization and nitrification along a wildfire-structured age gradient in chaparral. *Soil Biology and Biochemistry* 95, 87–99. doi:10.1016/j.soilbio.2015.12.017
- Hart SC, Nason GE, Myrold DD, Perry DA (1994) Dynamics of gross nitrogen transformations in an old-growth forest: the carbon connection. *Ecology* 75(4), 880–891. doi:10.2307/1939413
- Hart SC, DeLuca TH, Newman GS, MacKenzie MD, Boyle SI (2005) Post-fire vegetative dynamics as drivers of microbial community structure and function in forest soils. *Forest Ecology and Management* 220(1–3), 166–184. doi:10.1016/j.foreco.2005.08.012
- Heindel RC, Murphy SF, Repert DA, Wetherbee GA, Liethen AE, Clow DW, Halamka TA (2022) Elevated nitrogen deposition to fire-prone forests adjacent to urban and agricultural areas, Colorado Front Range, USA. *Earth's Future* 10(7), e2021EF002373. doi:10.1029/2021EF002373
- Hill AR (1996) Nitrate removal in stream riparian zones. *Journal of Environmental Quality* 25(4), 743–755. doi:10.2134/jeq1996.00472425002500040014x
- Johnson DW, Murphy JF, Susfalk RB, Caldwell TG, Miller WW, Walker RF, Powers RF (2005) The effects of wildfire, salvage logging, and post-fire N-fixation on the nutrient budgets of a Sierran forest. *Forest Ecology and Management* 220(1–3), 155–165. doi:10.1016/j.foreco.2005.08.011
- Jones MO, Allred BW, Naugle DE, Maestas JD, Donnelly P, Metz LJ, Karl J, Smith R, Bestelmeyer B, Boyd C, Kerby JD, McIver JD (2018) Innovation in rangeland monitoring: annual, 30 m, plant functional type percent cover maps for U.S. rangelands, 1984–2017. *Ecosphere* 9(9), e02430. doi:10.1002/ecs2.2430
- Jones MO, Robinson NP, Naugle DE, Maestas JD, Reeves MC, Lankston RW, Allred BW (2021) Annual and 16-Day rangeland production estimates for the Western United States. *Rangeland Ecology and Management* 77, 112–117. doi:10.1016/j.rama.2021.04.003
- Kampf SK, McGrath D, Sears MG, Fassnacht SR, Kiewiet L, Hammond JC (2022) Increasing wildfire impacts on snowpack in the western U.S.

- Proceedings of the National Academy of Sciences of the United States of America* 119(39), e2200333119. doi:10.1073/pnas.2200333119
- Kaufmann MR, Regan CM, Brown PM (2000) Heterogeneity in ponderosa pine/Douglas-fir forests: age and size structure in unlogged and logged landscapes of central Colorado. *Canadian Journal of Forest Research* 30(5), 698–711. doi:10.1139/x99-255
- Kaye JP, Hart SC, Fulé PZ, Covington WW, Moore MM, Kaye MW (2005) Initial carbon, nitrogen, and phosphorus fluxes following ponderosa pine restoration treatments. *Ecological Applications* 15(5), 1581–1593. doi:10.1890/04-0868
- Kurth VJ, Hart SC, Ross CS, Kaye JP, Fulé PZ (2014) Stand-replacing wildfires increase nitrification for decades in southwestern ponderosa pine forests. *Oecologia* 175(1), 395–407. doi:10.1007/s00442-014-2906-x
- Lane PNJ, Sheridan GJ, Noske PJ, Sherwin CB (2008) Phosphorus and nitrogen exports from SE Australian forests following wildfire. *Journal of Hydrology* 361(1–2), 186–198. doi:10.1016/j.jhydrol.2008.07.041
- Lowrance R, Vellidis G, Hubbard RK (1995) Denitrification in a restored riparian forest wetland. *Journal of Environmental Quality* 24(5), 808–815. doi:10.2134/jeq1995.00472425002400050003x
- Mansilha C, Melo A, Martins ZE, Ferreira IMPLVO, Pereira AM, Marques JE (2020) Wildfire effects on groundwater quality from springs connected to small public supply systems in a peri-urban forest area (Braga region, NW Portugal). *Water* 12(4), 1146. doi:10.3390/w12041146
- Mast MA, Murphy SF, Clow DW, Penn CA, Sexstone GA (2016) Water-quality response to a high-elevation wildfire in the Colorado Front Range. *Hydrological Processes* 30(12), 1811–1823. doi:10.1002/hyp.10755
- Mayer PM, Reynolds SK, McCutchen MD, Canfield TJ (2007) Meta-Analysis of nitrogen removal in riparian buffers. *Journal of Environmental Quality* 36(4), 1172–1180. doi:10.2134/jeq.2006.0462
- McClain ME, Boyer EW, Dent CL, Gergel SE, Grimm NB, Groffman PM, Hart SC, Harvey JW, Johnston CA, Mayorga E, McDowell WH, Pinay G (2003) Biogeochemical hot spots and hot moments at the interface of terrestrial and aquatic ecosystems. *Ecosystems* 6(4), 301–312. doi:10.1007/s10021-003-0161-9
- McGrath D, Zeller L, Bonnell R, Reis W, Kampf S, Williams K, Okal M, Olsen-Mikitowicz A, Bump E, Sears M, Rittger K (2023) Declines in peak snow water equivalent and elevated snowmelt rates following the 2020 Cameron Peak Wildfire in Northern Colorado. *Geophysical Research Letters* 50(6), 510–527. doi:10.1029/2022GL101294
- Mitsch WJ, Zhang L, Anderson CJ, Altor AE, Hernández ME (2005) Creating riverine wetlands: ecological succession, nutrient retention, and pulsing effects. *Ecological Engineering* 25(5), 510–527. doi:10.1016/j.ecoleng.2005.04.014
- Moody JA, Ebel BA (2012) Hyper-dry conditions provide new insights into the cause of extreme floods after wildfire. *Catena* 93, 58–63. doi:10.1016/j.catena.2012.01.006
- Moody JA, Martin DA (2001) Initial hydrologic and geomorphic response following a wildfire in the Colorado front range. *Earth Surface Processes and Landforms* 26(10), 1049–1070. doi:10.1002/esp.253
- Moore R (1992) 'Soil survey of Pike National Forest, Eastern Park, Colorado.' pp. 1–106. (USDA Forest Service and Soil Conservation Service)
- Murphy JD, Johnson DW, Miller WW, Walker RF, Carroll EF, Blank RR (2006) Wildfire effects on soil nutrients and leaching in a Tahoe Basin watershed. *Journal of Environmental Quality* 35(2), 479–489. doi:10.2134/jeq2005.0144
- Pierson DN, Robichaud PR, Rhoades CC, Brown RE (2019) Soil carbon and nitrogen eroded after severe wildfire and erosion mitigation treatments. *International Journal of Wildland Fire* 28(10), 814–821. doi:10.1071/WF18193
- Postila H, Heiderscheidt E (2020) Function and biomass production of willow wetlands applied in the polishing phase of sewage treatment in cold climate conditions. *Science of The Total Environment* 727, 138620. doi:10.1016/j.scitotenv.2020.138620
- Rhea AE, Covino TP, Rhoades CC, Brooks AC (2022) Use of geostatistical models to evaluate landscape and stream network controls on post-fire stream nitrate concentrations. *Hydrological Processes* 36(9), e14689. doi:10.1002/hyp.14689
- Rhoades CC (2018) Soil nitrogen leaching in logged beetle-killed forests and implications for riparian fuel reduction. *Journal of Environmental Quality* 48(2), 305–313. doi:10.2134/jeq2018.04.0169
- Rhoades CC, Entwistle D, Butler D (2011) The influence of wildfire extent and severity on streamwater chemistry, sediment and temperature following the Hayman Fire, Colorado. *International Journal of Wildland Fire* 20(3), 430–442. doi:10.1071/WF09086
- Rhoades CC, McCutchan JH, Cooper LA, Clow D, Detmer TM, Briggs JS, Stednick JD, Veblen TT, Ertz RM, Likensh GE, Lewis WM (2013) Biogeochemistry of beetle-killed forests: explaining a weak nitrate response. *Proceedings of the National Academy of Sciences of the United States of America* 110(5), 1756–1760. doi:10.1073/pnas.1221029110
- Rhoades CC, Chow AT, Covino TP, Fegél TS, Pierson DN, Rhea AE (2019) The legacy of a severe wildfire on stream nitrogen and carbon in headwater catchments. *Ecosystems* 22(3), 643–657. doi:10.1007/s10021-018-0293-6
- Rhoades CC, Fegél TS, Rhea AE, Heath J, Struthers S, Willi K, Ross MRV (2025a) Stream chemistry after Colorado's largest wildfire: solute-specific responses to ash and rainstorms. *Ecosystems* 28(5), 55. doi:10.1007/s10021-025-00997-2
- Rhoades CC, Fegél TS, Schneider C, Vorster AG (2025b) Post-fire seedling recruitment across a range of stand age in bark-beetle impacted lodgepole pine forests: Informing reforestation needs. *Forest Ecology and Management* 596, 123048. doi:10.1016/j.foreco.2025.123048
- Robinson NP, Allred BW, Smith WK, Jones MO, Moreno A, Erickson TA, Naugle DE, Running SW (2018) Terrestrial primary production for the conterminous United States derived from Landsat 30 m and MODIS 250 m. *Remote Sensing in Ecology and Conservation* 4(3), 264–280. doi:10.1002/rse2.74
- Robinson NP, Jones MO, Moreno A, Erickson TA, Naugle DE, Allred BW (2019) Rangeland productivity partitioned to sub-pixel plant functional types. *Remote Sensing* 11(12), 1427. doi:10.3390/rs11121427
- Rother MT, Veblen TT (2016) Limited conifer regeneration following wildfires in dry ponderosa pine forests of the Colorado Front Range. *Ecosphere* 7(12), e01594. doi:10.1002/ecs2.1594
- Ruleman CA, Bohannon RG, Bryant B, Shroba RR, Premo WR (2011) 'Geologic map of the Bailey 30' x 60' quadrangle, north-central Colorado'. Scientific Investigations Map SIM-3156, scale 1:100,000. (U.S. Geological Survey)
- Running SW, Nemani RR, Heinsch FA, Zhao M, Reeves M, Hashimoto H (2004) A continuous satellite-derived measure of global terrestrial primary production. *BioScience* 54(6), 547–560. doi:10.1641/0006-3568(2004)054[0547:ACSMOG]2.0.CO;2
- Rust AJ, Hogue TS, Saxe S, McCray J (2018) Post-fire water-quality response in the western United States. *International Journal of Wildland Fire* 27(3), 203–216. doi:10.1071/WF17115
- Shogren AJ, Zarnetske JP, Abbott BW, Iannucci F, Medvedeff A, Cairns S, Duda MJ, Bowden WB (2021) Arctic concentration-discharge relationships for dissolved organic carbon and nitrate vary with landscape and season. *Limnology and Oceanography* 66(S1), S197–S215. doi:10.1002/lno.11682
- Silverman NL, Allred BW, Donnelly JP, Chapman TB, Maestas JD, Wheaton JM, White J, Naugle DE (2019) Low-tech riparian and wet meadow restoration increases vegetation productivity and resilience across semiarid rangelands. *Restoration Ecology* 27(2), 269–278. doi:10.1111/rec.12869
- Smith HG, Sheridan GJ, Lane PNJ, Nyman P, Haydon S (2011) Wildfire effects on water quality in forest catchments: a review with implications for water supply. *Journal of Hydrology* 396(1–2), 170–192. doi:10.1016/j.jhydrol.2010.10.043
- Smithwick EAH, Kashian DM, Ryan MG, Turner MG (2009) Long-term nitrogen storage and soil nitrogen availability in post-fire lodgepole pine ecosystems. *Ecosystems* 12(5), 792–806. doi:10.1007/s10021-009-9257-1
- Stevens-Rumann CS, Morgan P (2019) Tree regeneration following wildfires in the western US: a review. *Fire Ecology* 15(1), 15. doi:10.1186/s42408-019-0032-1
- Stevens-Rumann CS, Kemp KB, Higuera PE, Harvey BJ, Rother MT, Donato DC, Morgan P, Veblen TT (2018) Evidence for declining forest resilience to wildfires under climate change. *Ecology Letters* 21(2), 243–252. doi:10.1111/ele.12889

- Stump LA, Binkley D (1992) Relationship between litter quality and nitrogen availability in Rocky Mountain forests. *Canadian Journal of Forest Research* 23(3), 492–502. doi:10.1139/x93-067
- Turner MG, Tinker DB, Romme WH, Kashian DM, Litton CM (2004) Landscape patterns of sapling density, leaf area, and aboveground net primary production in postfire lodgepole pine forests, Yellowstone National Park (USA). *Ecosystems* 7(7), 751–775. doi:10.1007/s10021-004-0011-4
- Turner MG, Smithwick EAH, Tinker DB, Romme WH (2009) Variation in foliar nitrogen and aboveground net primary production in young postfire lodgepole pine. *Canadian Journal of Forest Research* 39(5), 1024–1035. doi:10.1139/X09-029
- U.S. Department of Agriculture (2023) American Forests partners with USDA Forest Service to expand reforestation across national forests. *USDA Press Release*, 6 December. Available at <https://www.usda.gov/about-usda/news/press-releases/2023/12/06/american-forests-partners-usda-forest-service-expand-reforestation-across-national-forests>
- Vidon PGF, Hill AR (2004) Landscape controls on nitrate removal in stream riparian zones. *Water Resources Research* 40(3), 1–14. doi:10.1029/2003WR002473
- Vitousek PM, Melillo JM (1979) Nitrate losses from disturbed forests: patterns and mechanisms. *Forest Science* 25(4), 605–619. doi:10.1093/forestscience/25.4.605
- Wan S, Hui D, Luo Y (2001) Fire effects on nitrogen pools and dynamics in terrestrial ecosystems: a meta-analysis. *Ecological Applications* 11(5), 1349–1365. doi:10.1890/1051-0761(2001)011[1349:FEONPA]2.0.CO;2
- Williams AP, Livneh B, McKinnon KA, Hansen WD, Mankin JS, Cook BI, Smerdon JE, Varuolo-Clarke AM, Bjarke NR, Juang CS, Lettenmaier DP (2022) Growing impact of wildfire on western US water supply. *Proceedings of the National Academy of Sciences of the United States of America* 119(10), e2114069119. doi:10.1073/pnas.2114069119
- WRCC (2021) Daily total precipitation Cheesman, Colorado (Station 053102). Available at <https://wrcc.dri.edu/cgi-bin/rawMAIN.pl?coCCHE>

Data availability. The data used in this paper can be shared by the corresponding author upon request.

Conflicts of interest. The authors declare that they have no conflicts of interest.

Declaration of funding. We are grateful for financial support from the US Forest Service National Fire Plan (2016–2019) and the Joint Fire Sciences Program (14-1-06-11). A.R. was additionally supported by NASA Headquarters under the NASA Earth and Space Science Fellowship Program and by the Colorado Forest Restoration Institute through the Southwest Forest Health and Wildfire Prevention Act. T.C.'s time was additionally supported by NSF award EAR 2333030.

Acknowledgements. Sincere thanks to Tim Fegel of the Rocky Mountain Research Station for his contributions to field and laboratory work. The authors also thank Isaac Trujillo, Brian Orth, Lizzie Hereford and Noah Sievers for field assistance.

Author affiliations

^AColorado Forest Restoration Institute, Colorado State University, Fort Collins, CO, USA.

^BDepartment of Land Resources and Environmental Sciences, Montana State University, Bozeman, MT, USA.

^CU.S. Forest Service Rocky Mountain Research Station, Fort Collins, CO, USA.